

Knudsen number, ideal hydrodynamic limit for elliptic flow and QGP viscosity in $\sqrt{s_{NN}}=62$ and 200 GeV Cu+Cu/Au+Au collisions

A. K. Chaudhuri*

Variable Energy Cyclotron Centre, 1/AF, Bidhan Nagar, Kolkata 700 064, India

(Dated: September 28, 2010)

Taking into account of entropy generation during evolution of a viscous fluid, we have estimated inverse Knudsen number, ideal hydrodynamic limit for elliptic flow and QGP viscosity to entropy ratio in $\sqrt{s_{NN}}=62$ and 200 GeV Cu+Cu/Au+Au collisions. Viscosity to entropy ratio is estimated as $\eta/s = 0.17 \pm 0.10 \pm 0.20$, the first error is statistical, the second one is systematic. In a central Au+Au collision, inverse Knudsen number is $\approx 2.80 \pm 1.63$, which presumably small for complete equilibration. In peripheral collisions it is even less. Ideal hydrodynamic limit for elliptic flow is $\sim 40\%$ more than the experimental flow in a central collision.

PACS numbers: 47.75.+f, 25.75.-q, 25.75.Ld

Recent experiments at RHIC produced convincing evidences that a collective matter is created in Au+Au collisions [1–4]. The evidences come mainly from observing finite elliptic flow in non-central collisions, which is now regarded as a definitive signature of collective effect [5, 6]. Elliptic flow measure the azimuthal correlation of produced particles with respect to the reaction plane. It is also best understood in a collective model like hydrodynamics [7]. In a non-central collision, the reaction zone is spatially asymmetric. Differential pressure gradient convert the spatial asymmetry in to momentum asymmetry. Ideal hydrodynamics has been quite successful explaining a large part of the experimental elliptic flow [7]. However it is now realized that the experimentally measured scaling of integrated v_2 with multiplicity or with collision centrality is not in agreement with ideal hydrodynamics. While ideal hydrodynamics predicts approximate scaling [8], in experiments scaling is violated [9, 10]. As discussed in [11], violation of the scaling can be understood as an indication of incomplete thermalization. Ideal hydrodynamics require local thermal equilibration. Deviation from the local equilibrium can lead to a characteristic dependence of the eccentricity scaled elliptic flow on charged particles multiplicity. Degree of thermalization in the fluid produced in Au+Au collisions can be characterized by the dimensionless parameter, Knudsen number (K) [11]. By definition, inverse of the Knudsen number is the number of collisions per particles,

$$K^{-1} = \frac{\bar{R}}{\lambda} = \bar{R}n\sigma \quad (1)$$

where \bar{R} is the characteristic size of the system, n is the particle density and σ is the inter particle cross section. Validity of hydrodynamics require that $K^{-1} \gg 1$, so that large number of collisions can bring the system to local thermal equilibrium. The opposite limit, $K^{-1} \ll$

1 is the Knudsen regime where hydrodynamics become inapplicable. The simple formula,

$$\left(\frac{v_2}{\epsilon}\right)^{ex} = \left(\frac{v_2}{\epsilon}\right)^{ih} \frac{K^{-1}}{K^{-1} + K_0^{-1}}, \quad (2)$$

proposed in [11] give qualitatively correct behavior of the experimental elliptic flow. In the limit of small Knudsen number, experimental flow approaches the ideal hydrodynamic limit $\left(\frac{v_2}{\epsilon}\right)^{ih}$ with a correction linear in K . In the other extreme limit of large K , flow is proportional to the Knudsen number K . In Eq.2, K_0^{-1} is a number of the order of unity, whose precise value can be determined only from explicit transport calculations. From Monte-Carlo simulation of transport equations K_0 was estimated, $K_0 = 0.70 \pm 0.03$ [12]. In [11] it was argued that inverse of the Knudsen number K^{-1} can be determined from the experimental data, as it is proportional to $\frac{1}{S} \frac{dN}{dy}$, where $\frac{dN}{dy}$ is the total multiplicity density and S is a measure of the transverse area of the collision zone,

$$\frac{1}{K} = c_s \sigma \frac{1}{S} \frac{dN}{dy} \quad (3)$$

In Eq.3, c_s is the speed of sound of the medium and σ is the inter-particle cross section. Eq.2 and 3 connect two experimental observables, elliptic flow and particle multiplicity and can be used to determine unknown quantities e.g. ideal hydrodynamic limit of elliptic flow $\left(\frac{v_2}{\epsilon}\right)^{ih}$, the combination of parameters $K_0 \sigma c_s$.

However, there is a serious flaw in the derivation of Eq.3 and the conclusions derived from it could be misleading. Eq.3 was obtained with the assumption that the total particle number is conserved throughout the evolution [11]. The assumption is justified in an isentropic expansion, i.e. one dimensional evolution of ideal fluid, when entropy density (s) times the proper time (τ) is a constant. Under such condition, $\frac{1}{S} \frac{dN}{dy} \propto s\tau \approx n\tau$ [13]. However, in a viscous evolution, entropy is generated and initial and final state entropy are not same and the assumption is clearly violated. Only in systems with very

*E-mail: akc@veccal.ernet.in

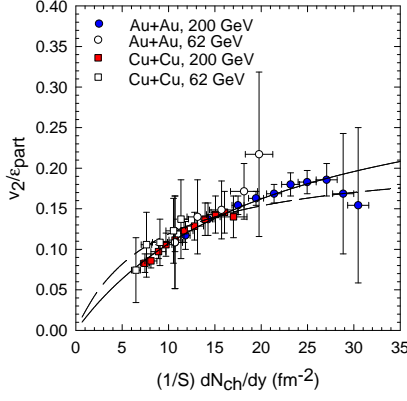


FIG. 1: (color online) PHOBOS data for the centrality dependence of eccentricity scaled elliptic flow in Cu+Cu and Au+Au collisions at $\sqrt{s_{NN}} = 62$ and 200 GeV. The solid line is the fit to the data with $(\frac{v_2}{\epsilon})^{ih} = 0.33$ and $(\frac{1}{\tau_i T_i} \frac{\eta}{s}) = 0.83$. The dashed line is the fit in the ideal fluid approximation, $(\frac{v_2}{\epsilon})^{ih} = 0.19$ and $(\frac{1}{\tau_i T_i} \frac{\eta}{s}) = 0$.

small viscosity, the assumption may be approximately valid, but not in systems where sufficient entropy is generated. Explicit numerical simulations indicate that in Au+Au collisions, entropy generation can be substantial, e.g. $\sim 20\%$, 30% and 50% in fluid evolution with viscosity to entropy ratio, $\eta/s = 0.08, 0.12$ and 0.16 [14]. One may argue that unlike in explicit numerical simulation of viscous hydrodynamics, Knudsen number ansatz does not require the entire dynamic range of evolution. Time of validity of Knudsen number ansatz is $\tau < \bar{R}/c_s$ [11]. For $c_s = \sqrt{1/3}$, and characteristic size $\bar{R} \approx 1-2$ fm, the time scale is $\tau < 1.7-3.5$ fm. Though the time scale is small compared to the entire dynamic range of evolution, it is large enough for significant entropy generation. In explicit simulation of viscous hydrodynamics, entropy generation is fast and most of the entropy is generated with first 2-4 fm of evolution [15]. Thus even though Knudsen number ansatz does not require full dynamic range of evolution, in the time scale for validity of Knudsen ansatz most of the entropy will be generated.

In the present paper accounting for the entropy generation in viscous evolution, we generalise Eq.3. As in [11], we also consider one dimensional Bjorken longitudinal expansion. If η and ζ is the shear and bulk viscosity coefficients, for Bjorken flow, energy-momentum conservation equation, $\partial_\mu T^{\mu\nu} = 0$ reduces to [16, 17],

$$\frac{d(s\tau)}{d\tau} = \frac{1}{\tau T} \left(\frac{4}{3} \eta + \zeta \right) \quad (4)$$

where s is the entropy density and τ is the proper time. In general bulk viscosity is much less than the shear viscosity, however, near the phase transition region bulk viscosity can be large [18, 19]. In the following we neglect the bulk viscosity. We further assume that shear viscosity is proportional to cube of the temperature. For

$\eta \propto T^3$, Eq.4 can be analytically integrated between time τ_i and τ_f . For $\tau_f \gg \tau_i$, the final state entropy can be written as [16, 17],

$$\tau_f s_f \approx \tau_i s_i \left[1 + \frac{2}{3\tau_i T_i} \left(\frac{\eta}{s} \right) \right]^3 \quad (5)$$

In Eq.5, T_i is the temperature at the time scale τ_i . Equating final state entropy density s_f with particle multiplicity per unit transverse area (S), $\tau_f s_f \approx 3.6 \frac{1}{S} \frac{dN}{dy}$ [13], we obtain the particle density at the time scale τ_i as,

$$n_i \approx \frac{1}{\tau_i} \frac{1}{S} \frac{dN}{dy} \left[1 + \frac{2}{3\tau_i T_i} \left(\frac{\eta}{s} \right) \right]^{-3} \quad (6)$$

Inserting Eq.6 in Eq.1, in the time scale $\tau_i \leq \bar{R}/c_s$, i.e. as long as the transverse size of the system does not vary significantly [11], inverse of Knudsen number can be obtained as,

$$\frac{1}{K} \approx \sigma c_s \left[\frac{1}{S} \frac{dN}{dy} \right] \left[1 + \frac{2}{3\tau_i T_i} \left(\frac{\eta}{s} \right) \right]^{-3} \quad (7)$$

One immediately observes that neglect of entropy generation during evolution will over estimate K^{-1} , by the factor $\left[1 + \frac{2}{3\tau_i T_i} \left(\frac{\eta}{s} \right) \right]^3$. As it will be shown below, experimental data indicate that the factor could be large, $\sim 2-7$.

Inserting Eq.7 in Eq.2, eccentricity scaled elliptic flow now can be related to observed particle multiplicity as,

$$\left(\frac{v_2}{\epsilon} \right)^{ex} = \left(\frac{v_2}{\epsilon} \right)^{ih} \frac{\frac{1}{S} \frac{dN}{dy} \left[1 + \frac{2}{3\tau_i T_i} \left(\frac{\eta}{s} \right) \right]^{-3}}{\frac{1}{K_0 \sigma c_s} + \frac{1}{S} \frac{dN}{dy} \left[1 + \frac{2}{3\tau_i T_i} \left(\frac{\eta}{s} \right) \right]^{-3}} \quad (8)$$

Experimental data on elliptic flow and particle multiplicity can be fitted with Eq.8 to obtain estimates of the hydrodynamic limit of elliptic flow $(\frac{v_2}{\epsilon})^{ih}$ and viscosity to entropy ratio in unit of initial time and temperature $(\frac{1}{\tau_i T_i} \frac{\eta}{s})$. Eq.8 also involve the quantity $K_0 \sigma c_s$. K_0 , σ and c_s are known approximately. For example, inter parton cross section is expected to be small, $\sigma = 3-4$ mb. From transport calculations, K_0 was estimated as $K_0 = 0.7 \pm 0.3$. The speed of sound of QGP medium is expected to be $c_s \approx \sqrt{1/3}$. In the following, we fix $\sigma = 3$ mb, $K_0 = 0.7$ and $c_s = \sqrt{1/3}$.

In Fig.1, PHOBOS [20–22] data for the centrality dependence of (participant) eccentricity scaled charged particles elliptic flow, in Au+Au and Cu+Cu collisions at $\sqrt{s_{NN}} = 62$ and 200 GeV are shown. PHOBOS data have large error bars and within the error data do not show any system size or energy dependence. All the

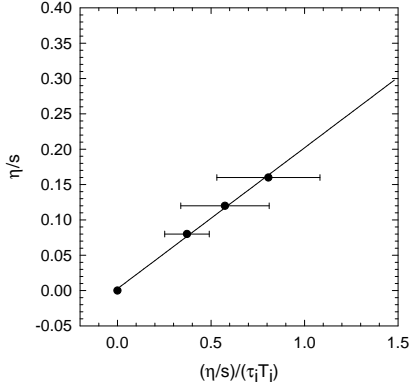


FIG. 2: Viscosity to entropy ratio η/s as a function of the parameter $\left(\frac{1}{\tau_i T_i} \frac{\eta}{s}\right)$ from the analysis in [14]. The solid line is a straight line fit.

four data sets are fitted together with Eq.8. The solid line in Fig.1 shows the fit. Data are well explained, χ^2 value is also small, $\chi^2/N \approx 0.1$. However, $\left(\frac{v_2}{\epsilon}\right)^{ih}$ and $\left(\frac{1}{\tau_i T_i} \frac{\eta}{s}\right)$ can be determined only with large uncertainties, $\left(\frac{v_2}{\epsilon}\right)^{ih} = 0.33 \pm 0.12$, $\left(\frac{1}{\tau_i T_i} \frac{\eta}{s}\right) = 0.83 \pm 0.51$. Uncertainty in $\left(\frac{v_2}{\epsilon}\right)^{ih}$ and $\left(\frac{1}{\tau_i T_i} \frac{\eta}{s}\right)$ would be reduced with better quality data. While definitive conclusions cannot be made due to large uncertainty in $\left(\frac{v_2}{\epsilon}\right)^{ih}$, the central value suggests that even in central Au+Au collisions, ideal hydrodynamic limit is not reached. In central/mid-central collisions, experimental flow is only $\sim 60\%$ of the ideal fluid limit. In peripheral collisions, it is even less. For comparison purpose, in Fig.1, we have shown the fit to the data in the ideal fluid approximation, $\left(\frac{1}{\tau_i T_i} \frac{\eta}{s}\right) = 0$. In the ideal fluid approximation ideal hydrodynamic limit for elliptic flow is estimated as, $\left(\frac{v_2}{\epsilon}\right)^{ih} = 0.19 \pm 0.04$. However, description to the data is comparatively poor, $\chi^2/N \approx 1.3$ is ~ 10 times larger than that obtained in viscous evolution.

With the estimate of $\left(\frac{1}{\tau_i T_i} \frac{\eta}{s}\right)$, we can compute inverse Knudsen number from Eq.7. In table.I, we have listed K^{-1} for different centrality ranges of Au+Au collisions. Particle multiplicities are taken from the PHOBOS data [20–22]. For comparison, we have also listed the values in the ideal fluid approximation. K^{-1} decreases by a factor of 2-7 when entropy generation is accounted for. In the ideal fluid approximation, $K^{-1} \approx 8$ in a central collision. It is reduced to ~ 2.8 if entropy generation during evolution is accounted for. While it is debatable whether $K^{-1} \approx 8$ can lead to complete equilibration, it is unlikely that complete thermalization will be achieved with $K^{-1} \approx 2.8$. In more peripheral collisions, equilibration is certainly incomplete.

QGP viscosity is an important parameter characterizing QGP medium. String theory based models (ADS/CFT) give a lower bound on viscosity to entropy

TABLE I: Inverse Knudsen number (K^{-1}), in ideal and viscous fluid, as a function of collision centrality in Au+Au collision. Also listed are charged particles multiplicity per unit transverse area ($\frac{1}{S} \frac{dN_{ch}}{dy}$) from PHOBOS experiment [20–22] and characteristic size \bar{R} of the system. Inter parton cross section is assumed to be $\sigma = 3$ mb, speed of sound $c_s = \sqrt{1/3}$.

collision centrality(%)	$\frac{1}{S} \frac{dN_{ch}}{dy}$ (fm^{-2})	\bar{R} (fm)	K^{-1}	
			$\left(\frac{1}{\tau_i T_i} \frac{\eta}{s}\right) = 0.83 \pm 0.51$	$\left(\frac{1}{\tau_i T_i} \frac{\eta}{s}\right) = 0$
0-3	30.46	2.01	2.80 ± 1.63	7.91
3-6	28.84	1.93	2.65 ± 1.55	7.49
6-10	27.06	1.84	2.49 ± 1.45	7.03
10-15	24.95	1.75	2.29 ± 1.33	6.48
15-20	23.17	1.64	2.13 ± 1.24	6.02
20-25	21.39	1.55	1.97 ± 1.15	5.56
25-30	19.44	1.45	1.79 ± 1.04	5.05
30-35	17.50	1.38	1.61 ± 0.94	4.55
35-40	14.26	1.30	1.31 ± 0.76	3.70
40-45	11.83	1.23	1.09 ± 0.63	3.07
45-50	10.69	1.18	0.98 ± 0.57	2.78

TABLE II: Listed are some estimates of QGP viscosity to entropy ratio from experimental data in Au+Au collisions at RHIC. The observables analyzed are also listed.

Sl. no.	$4\pi\eta/s$	Experimental observable
1	$0.88 \pm 0.38 \pm 1.76$	ϕ meson's $\langle N \rangle$, $\langle p_T \rangle$ and v_2 [14]
2	1.0-3.77	p_T fluctuations [26]
3	1.4-2.4	v_2 scaling violation [27]
4	≈ 2	v_2 scaling violation [28]
5	$1.13 \pm 0.19 \pm 1.26$	v_2 scaling violation [29]
6	1.51 ± 0.38	v_2 scaling violation [30]
7	1.3-2.0	heavy quark energy loss [31]
8	1.45 ± 0.06	v_2 [32]
9	≤ 1.51	p_T spectra of π , K and p [33]
10	$2.14 \pm 1.26 \pm 2.56^a$	v_2 & $\frac{1}{S} \frac{dN_{ch}}{dy}$

^apresent work

ratio of any matter, $4\pi\eta/s \geq 1$ [23]. In [24, 25], from experimental data, a phenomenological upper bound was conjectured, $4\pi\eta/s < 5$. We have obtained viscosity to entropy ratio in unit of initial time and temperature. It can be converted to more comprehensible viscosity to entropy ratio if the initial time and temperature scale is known. Recently, in [14] STAR data on ϕ mesons multiplicity, mean p_T and integrated v_2 were analyzed in ideal and viscous fluid dynamics. At the initial time $\tau_i = 0.6$ fm, ideal or viscous fluid was initialized to reproduce experimental ϕ meson multiplicity. Viscous fluid requires less initial temperature than an ideal fluid. Results of the analysis are shown in Fig.2, where η/s as a func-

tion of the parameter $\left(\frac{1}{\tau_i T_i} \frac{\eta}{s}\right)$ is shown. The solid line in Fig.2 is a straight line fit, $\eta/s = 0.2 \left(\frac{1}{\tau_i T_i} \frac{\eta}{s}\right)$. The relation can be used to convert extracted $\left(\frac{1}{\tau_i T_i} \frac{\eta}{s}\right)$ to η/s . We obtain, $\eta/s = 0.17 \pm 0.10$. From the PHOBOS data, viscosity to entropy ratio can be determined only within $\sim 60\%$ accuracy. Evidently, much better quality data are required for more precise determination of viscosity to entropy ratio. As mentioned earlier, the estimate was obtained with $K_0 = 0.7$, $c_s = \sqrt{1/3}$ and $\sigma = 0.3 fm^2$ corresponding to, $K_0 \sigma c_s \approx 0.121$. Estimate of viscosity depend on the value of $K_0 \sigma c_s$. Systematic uncertainty in η/s is $\sim 120\%$ due to a factor of 2 uncertainty in $K_0 \sigma c_s$. We then estimate QGP viscosity to entropy ratio as $\eta/s = 0.17 \pm 0.10 \pm 0.20$, the first error is statistical, the second is systematic. Systematic uncertainty will increase if uncertainty in initial time and temperature scale is included. The estimated value is well with the two bounds, $1 \leq 4\pi\eta/s \leq 5$ [23–25]. In table.II, present estimate for QGP viscosity is compared with some recent estimates. One may note that presently estimated η/s is similar to the values obtained in previous extractions [27],[28], which disregarded entropy generation in the Knudsen ansatz. The reason is understood. Experimental data include the effect of entropy generation. Thus even if viscous effects are neglected in the Knudsen ansatz, the fitted parameters $\left(\frac{v_2}{\epsilon}\right)^{ih}$ and $K_0 \sigma c_s$

(see Eq.8) will include the effect.

We note that the present estimate should be considered as an upper limit for QGP viscosity. We have neglected bulk viscosity. Experimental data include the effect of bulk viscosity. Neglect of bulk viscosity will be compensated by increasing η/s . Also, we have neglected transverse expansion. Experimental data also include the effect of transverse expansion. One observes from Eq.7 that K^{-1} will decrease if transverse expansion is included (transverse area of system at freeze-out will be larger than the initial area). Neglect of the transverse expansion will be compensated again by increasing η/s .

To conclude, taking into account that entropy is generated during evolution of a viscous fluid, we have generalized a relation between inverse Knudsen number K^{-1} and particle density $\frac{1}{S} \frac{dN}{dy}$. PHOBOS data on the centrality dependence of elliptic flow indicate that K^{-1} is overestimated by a factor $\sim 2-7$ if entropy generation is neglected. We have also estimated ideal hydrodynamic limit for elliptic flow $\left(\frac{v_2}{\epsilon}\right)^{ih}$ and QGP viscosity to entropy ratio η/s . Estimated $\left(\frac{v_2}{\epsilon}\right)^{ih}$ is $\sim 40\%$ larger than the scaled flow in a central collision. Estimated viscosity to entropy ratio, $4\pi\eta/s = 2.14 \pm 1.26$ is well within the ADS/CFT lower bound and phenomenological upper bound, $1 \leq 4\pi\eta/s \leq 5$.

-
- [1] BRAHMS Collaboration, I. Arsene *et al.*, Nucl. Phys. A **757**, 1 (2005).
 - [2] PHOBOS Collaboration, B. B. Back *et al.*, Nucl. Phys. A **757**, 28 (2005).
 - [3] PHENIX Collaboration, K. Adcox *et al.*, Nucl. Phys. A **757** 184 (2005).
 - [4] STAR Collaboration, J. Adams *et al.*, Nucl. Phys. A **757** 102 (2005).
 - [5] J. Y. Ollitrault, Phys. Rev. D **46**, 229 (1992).
 - [6] A. M. Poskanzer and S. A. Voloshin, Phys. Rev. C **58**, 1671 (1998).
 - [7] P. F. Kolb and U. Heinz, in *Quark-Gluon Plasma 3*, edited by R. C. Hwa and X.-N. Wang (World Scientific, Singapore, 2004), p. 634.
 - [8] H. Song and U. W. Heinz, Phys. Rev. C **78**, 024902 (2008).
 - [9] S. A. Voloshin [STAR Collaboration], J. Phys. G **34**, S883 (2007).
 - [10] S. A. Voloshin [STAR Collaboration], AIP Conf. Proc. **870**, 691 (2006).
 - [11] R. S. Bhalerao, J. P. Blaizot, N. Borghini and J. Y. Ollitrault, Phys. Lett. B **627**, 49 (2005).
 - [12] C. Gombeaud and J. Y. Ollitrault, Phys. Rev. C **77**, 054904 (2008).
 - [13] R. C. Hwa and K. Kajantie, Phys. Rev. D **32**, 1109 (1985).
 - [14] A. K. Chaudhuri, Phys. Lett. B **681**, 418 (2009).
 - [15] A. K. Chaudhuri, Phys. Rev. C **74**, 044904 (2006).
 - [16] P. Danielewicz and M. Gyulassy, Phys. Rev. D **31**, 53 (1985).
 - [17] A. Muronga, Phys. Rev. Lett. **88**, 062302 (2002) [Erratum-ibid. **89**, 159901 (2002)].
 - [18] D. Kharzeev and K. Tuchin, JHEP **0809**, 093 (2008).
 - [19] F. Karsch, D. Kharzeev and K. Tuchin, Phys. Lett. B **663**, 217 (2008).
 - [20] B. B. Back *et al.* [PHOBOS Collaboration], Phys. Rev. C **72**, 051901 (2005).
 - [21] B. Alver *et al.* [PHOBOS Collaboration], Phys. Rev. Lett. **98**, 242302 (2007).
 - [22] B. Alver *et al.*, Phys. Rev. C **77**, 014906 (2008).
 - [23] G. Policastro, D. T. Son and A. O. Starinets, Phys. Rev. Lett. **87**, 081601 (2001).
 - [24] M. Luzum and P. Romatschke, Phys. Rev. C **78**, 034915 (2008).
 - [25] H. Song and U. W. Heinz, J. Phys. G **36**, 064033 (2009).
 - [26] S. Gavin and M. Abdel-Aziz, Phys. Rev. Lett. **97**, 162302 (2006).
 - [27] H. J. Drescher, A. Dumitru, C. Gombeaud and J. Y. Ollitrault, Phys. Rev. C **76**, 024905 (2007).
 - [28] H. Masui, J. Y. Ollitrault, R. Snellings and A. Tang, Nucl. Phys. A **830**, 463C (2009).
 - [29] R. A. Lacey *et al.*, Phys. Rev. Lett. **98**, 092301 (2007).
 - [30] A. K. Chaudhuri, Phys. Rev. C **81**, 044905 (2010).
 - [31] A. Adare *et al.* [PHENIX Collaboration], Phys. Rev. Lett. **98**, 172301 (2007).
 - [32] A. K. Chaudhuri, J. Phys. G **37**, 075011 (2010).
 - [33] V. Roy and A. K. Chaudhuri, arXiv:1003.1195 [nucl-th].